Effects of the electron–hole pair in Auger and X-ray photoemission spectroscopy from surfaces of Fe–Si

CrossMark

J.L. Gervasoni [a,1,*], M. Jenko [b], B. Poniku [b], I. Belič [b], A. Juan [c,1]

[a] Centro Atomico Bariloche and Instituto Balseiro, Comision Nacional de Energia Atomica, Universidad Nacional de Cuyo, R8402AGP S. C. de Bariloche, Rio Negro, Argentina
[b] Institute of Metals and Technology, Lepi pot 11, 1000 Ljubljana, Slovenia
[c] Departamento de Física, Universidad Nacional del Sur, Bahia Blanca, Argentina

ABSTRACT

In this work, we investigate in detail the effects due to the interaction between an electron and a stationary positive ion (or atomic hole) in the neighborhood of a surface of Fe–Si, having a strong plasmon peak in their electron energy loss spectra, when it is excited with synchrotron radiation. We take into account the effects due to the sudden creation of an electron and the residual holes, one in the case of X-ray photoemission spectroscopy (XPS) and two in the case of Auger electron spectroscopy (AES).

We use a semi classical dielectric formulation for the photoelectron trajectory, and we estimated the parameter r_s, the radius of the sphere occupied by one electron in the solid, which is critical in order to define the electron density of the alloy. With the cited formulation, we have obtained a detailed behavior of the different contributions of the collective excitations in both processes.

© 2015 Elsevier B.V. All rights reserved.

1. Introduction

In the field of spectroscopic analysis, there has been a continuing interest concerning the properties of interfaces and solid surfaces, particularly when looking at their interactions with charged particles and radiation. These properties and interactions are important, e.g., in heterogeneous catalysis, in various applications of semiconductors and thin films, or in corrosion protection. As a result, an intense development of different methods and tools for studying surfaces has recently taken place. Applications of electron spectroscopies for analysis of surfaces and interfaces have a very significant impact on the progress of this field [1–7].

The behavior of an emitted electron with an ion near the surface is of interest to understand the effects of the simultaneous dynamic interaction of electron, ion and surface involved in the spectra obtained in high scattering experiments.

The purpose of this paper is to investigate in detail the effect of the interaction between a fast emitted electron and a stationary (or atomic hole) ion in Fe–Si compounds. In particular, we study how creating a positive charge localized on the solid can influence the inelastic energy dissipation of the electron, and the corresponding spectra. It is well known [2] that there are two different

contributions to the main interaction of external charged particle electron gas with the material: the individual excitations (electron-particle external) and collective (plasmon oscillation). This last contribution is to be discussed in detail in this paper.

We analyze the interaction of the sudden creation of the electron–hole pair with solid interfaces of Fe–Si compounds, in terms of the dielectric formalism and the semi-classical approach, using the so-called surface reflection model [1–3]. This model has been quite useful for applications in studies of particles-surfaces interaction processes, as well as in the field of electromagnetism [4].

Although in general, the surfaces are well defined to a macroscopic level, they usually present roughness at atomic scale that make their treatment difficult. In the following we will constrain ourselves to the study of smooth surfaces. This limitation must be taken into account when comparing with experimental results.

Turning to the problem established by the non-invariant translational of the dielectric function that characterizes the solid, we consider that the photo-electron follows a well-defined classical trajectory, exciting collective oscillations in the bulk and on the surface [1]. In this mechanism of plasmon excitation it loses energy, which depend of the material that it travel as well as of its initial energy (or velocity).

In principle, the formalism that we developed in previous works [7–9] can be applied in different electron spectroscopies (i.e., AES, UPS and XPS). In this work we study the difference in the energy loss of the photoelectron and the Auger electron between both

---

* Corresponding author.
[1] Member of Consejo Nacional de Investigaciones Cientificas y Tecnicas (CONICET), Argentina.

XPS and AES processes, and the difference in the corresponding probabilities of bulk and surface plasmon excitations.

We apply our formalism for the final state of the Auger process: two holes and an emerging electron all interacting with the electron gas and contributing to the electron energy loss. The new contribution to this research is that we apply our previous results to a solid form with two pure elements.

In Section 2, we give a brief account of the method used for the calculation of the energy loss of the particle in both processes within the solid appearing because of the sudden creation of the electron–hole pair, and as a result of the transport of the photo- or Auger electron in the medium.

In Section 3, we present the results of our calculations for the alloy Fe–Si.

In Section 4, we discuss the main features of our results and finally in Section 5 we summarize the work and comment on some perspectives for further research.

2. Theoretical description

In order to investigate the energy loss of a photoelectron due to plasmon excitation we use a semiclassical model developed in previous works [7–9], as well as the dielectric response model used by Yubero and Tougaard [10].

The whole system involved: the hole (one hole for XPS and two for AES) and the electron are created at a distance z_0 from the interface between the metal and the vacuum. We assume that the hole is fixed at $\boldsymbol{r}_0 = (0, z_0)$ while the emitted electron with velocity $\boldsymbol{u}$ follows a uniform trajectory $\boldsymbol{r}_e = \boldsymbol{r}_0 + \boldsymbol{u}t$, perpendicular to the surface, which remains undisturbed by the plasmon excitation events. This approximation holds for sufficiently large kinetic energies, $mu^2/2 \gg \hbar\omega_p$ [11–18]. Within our formalism, this approach is fully justified: in X-ray photoemission spectroscopy (XPS) and in X-ray excited Auger electron spectroscopy (AES) the energy of the emitted electron is in the several hundred eV or in the keV range, while $\hbar\omega_p$ is lower, than 20–25 eV.

2.1. Some considerations on the Auger process

This is more complicated to handle in the sense that it can be considered a several-level process: the first occurs when a primary electron creates an initial hole in some internal shell of the atom. In a second instance both primary electron and core electron leave the atom with a more or less defined energy. This is because the escaping primary electron suffers scattering processes and the electronic structure of the ionised atom is rearranged. This rearrangement, which is a third stage in the process, is done in such a way that after a time of the order of 10^{-15} s, the deep initial hole in the core level is filled by an electron originating from an energetically higher-lying shell. This transition may be accompanied by the emission of a characteristic X-ray photon (we have not taken into account this case), or alternatively the deexcitation process might be a radiationless Auger transition, in which the energy lost by the electron that falls into the deeper atomic level is transferred to another electron of the same or a different shell. Simultaneously, this latter electron is then emitted with a characteristic Auger energy, leaving the atom in a doubled-ionised state (two holes in different or same core levels) [19]. It is in this last level that we apply our formalism: two holes and an emerging electron all interacting with the electron gas and contributing to the average number of plasmon excitations.

We use the so called specular reflection model [2] to describe the system and the involved field. In this frame, the behavior of the material is given by the local dielectric function [2]:

$$\varepsilon(k, \omega) = \varepsilon(\omega) = 1 - \omega_p^2 / \omega(\omega + i\gamma), \tag{1}$$

with the corresponding values for the plasma frequency ω_p and the damping constant γ. Throughout the paper we use atomic units.

ω_p is related to r_s as:

$$\omega_p^2 = 4\pi \eta q e^2 / m, \tag{2}$$

where η is the electronic density and m is the electron mass [14].

In the so-called jellium model the solid is replaced by a homogeneous electron gas and a background of positive charges with the same average density in order to maintain the system's neutrality. The fundamental parameter of the model is r_s (u.a.), which is defined as the radius of the sphere occupied by one electron in the solid. This quantity is related with the electronic density and this with the dielectric function.

The dependence of r_s from η is:

$$\eta^{-1} = 4\pi / 3 r_s^3 \tag{3}$$

Hence, according to the specular reflection model, the charge densities of the moving electron q_- and the static positive charge q_+ are

$$\rho_{q_-}(\boldsymbol{r}, t) = q_- \delta(\boldsymbol{r} - \boldsymbol{u}) H_1(t)$$
$$\rho_{q_+}(\boldsymbol{r}, t) = q_+ \delta(\boldsymbol{r} - \boldsymbol{r}_0) H_1(t)$$

where $H_1(t)$ is the Heaviside function and $\boldsymbol{r}$ is the radial coordinate.

Following the dielectric formalism and specular reflection model, developed in Ref. [7], the induced potentials in the medium (M) and the vacuum (V) are given by:

$$\phi_{ind}^M(k, \omega) = F_{q_-}^{M,b} + F_{q_-}^{M,s} + F_{q_+}^{M,b} + F_{q_+}^{M,s} \tag{4a}$$
$$\phi_{ind}^V(k, \omega) = F_{q_-}^{V,s} + F_{q_+}^{V,s}, \tag{4b}$$

where analytical expressions for the F functions are given in the Appendix A.

Remembering that the energy loss due to plasmon excitation is:

$$dW/dt = Zq. \partial \Phi_{ind}(\boldsymbol{r}, t) / \partial t |_{\boldsymbol{r} = z + \boldsymbol{v}t}$$

where $\Phi_{ind}(\boldsymbol{r},t)$ is the potential induced in the medium by the external charges (electron plus holes) [7–9], the total energy dissipation rate due to the fields acting on the emitted electron is:

$$\dot{W}_{dis}^{(q)} = Zq \frac{\partial \phi_{ind}(\boldsymbol{r}, t)}{\partial t}$$
$$= -iZq \int \frac{d^3 \boldsymbol{k}}{(2\pi)^3} \int \frac{d\omega}{2\pi} \omega \phi_{ind}(\boldsymbol{k}, \omega) e^{i(\boldsymbol{k}.\boldsymbol{r} - \omega t)} \Bigg|_{\boldsymbol{r} = \boldsymbol{r}_Z(t)} \tag{5}$$

where Zq is the charge of the external particle (hole or electron). Here $q = -e$ for the electron, $q = e$ for the photoionization and $q = 2e$ for the Auger process for the charge of the hole.

3. Results

In order to characterize the alloy we have to obtain the parameter r_s of it. As the electronic density is dependent of the parameter r_s, it is critical to determine it for the alloy as a whole.

From Eq. (2) the plasma frequency of the alloy was determined establishing a relationship between the composition of the alloy and plasma frequencies of the pure materials that compose it.

That is, according to this Eq. as follows:

$$\omega_p^{FeSi} = (\%Fe). \omega_p^{Fe} pFe + (\%Si). \omega \omega_p^{Si} \tag{6}$$

(with % meaning either the atomic or weight percentage).

We have to noticed that much experimental evidence will be necessary to find a simple relationship linking ω_p with the composition, such as the measurement on Fe–Si films with different
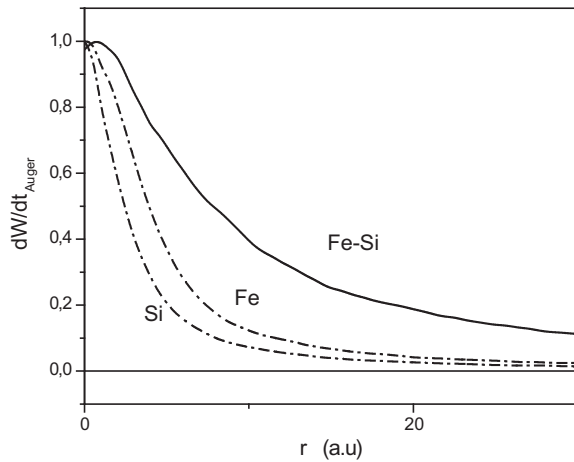
Fig. 1. Energy loss in Auger process for a photoelectron traveling pure Si and Fe, comparing with the Fe–Si alloy.

Fig. 2. Dimensionless electronic bulk density ρ excited due to AES (points) and XPS (continued line) processes vs. dimensionless characteristic distance from the surface of Fe–Si alloy. The emitted electron has a velocity $v = 4$ a.u. C_∞ is the concentration of the solute at infinite dilution and $\beta = r_s^{Fe}/r_s^{Si}$ is the rate of the parameter r_s of each element of the alloy.

percentages of Fe and Si, and also taking into account the thermodynamic characteristics of each composition of the alloy such as the formation and stability of phases, the diffusion of the compounds in the matrix, the structure with which the alloy is formed, etc. The present work is only a first approximation to the problem, where these variables have not yet been incorporated. In this system the solubility of silicon in iron is very low (it is at most 11at.%). It is also an alloy with no metastable intermetallic phases. Moreover, the diffusion of alloying does not seem to be something to consider since, although iron is a metal whose melting point is low compared with other metals, diffusive processes in Fe–Si are around 550 °C [15]. Since the analysis was carried out at room temperature, silicon diffusion into the matrix of Fe was not taken into account.

Replacing Eq. (2) in Eq. (3), we obtain for the Fe–Si alloy: $r_s^{Fe–Si} = 4.57$ a.u.

Finally, we have the energy loss due to plasmon excitations, taking into account the contribution of the electron (e), its image (e'), the hole (h) and its image (h'):

$$\left.\frac{dW}{dt}\right|_\mu = dW/dt|_{\mu e} + dW/dt|_{\mu h} + dW/dt|_{\mu e'} + dW/dt|_{\mu h'}, \qquad (7)$$

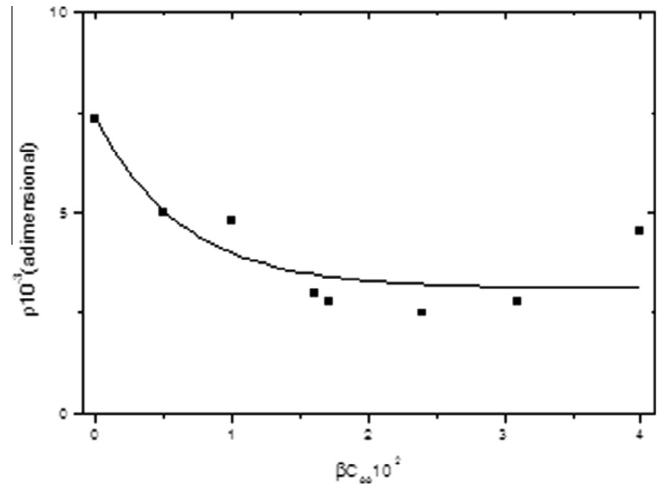being μ: Auger or XPS process.

In order to compare both (X-ray photoemission and Auger electron emission), we consider only internal emission, following the development did in Refs. [19–22], applying our results to Fe–Si alloy.

We evaluate the time dependence of dW/dt (Eq. (7)) for an electron emitted with a velocity $u = 4$ a.u. The electron–hole pair is created at a depth $\boldsymbol{r} = \boldsymbol{r}_0 = 0$ inside the metal. We replace the induced potential of Eqs. (4a) and (4b) in the energy loss (Eq. (7)).

In Fig. 1 we plot different cases of Auger process, corresponding to pure Fe and Si, comparing with the compound formed by these two elements.

In studies of electron emission in XPS, the contribution of the pure and alloy elements are quite similar to Auger contributions.

In Fig. 2 we show the results of electronic density for the Fe–Si alloy. It is interesting to observe that the importance of the hole is neglectable with respect to the elements Fe and Si separately. It is only due to the effect of the two final state holes in the Auger process (however, these differences do not depend on the energy of the emitted electron).

4. Concluding remarks

In summary, we have used the dielectric function formalism and the specular reflection model, together with the pseudo-extended medium, for comparing the excitation of plasmons during the emission of electrons in the proximity of a solid surface of a Fe–Si alloy, in order to investigate in detail the different contributions to the processes of photoemission and Auger electron emission, comparing with the pure elements Fe and Si.

Our results for the energy loss and electronic density show that this particular alloy can be treated using the same approximation as for the pure elements Fe (metal) and Si (semiconductor). For the case of excitation of plasmons the single-pole approximation can be used, although with a finite damping [23]. Moreover, we note that our general formulation of the problem through the dielectric approach also enables the study of the effects arising from different response functions (different materials).

From this result, we find some novel structures that are under discussion.

The method described here is useful for studying multiple plasmon excitations and for understanding the electron spectra excited from these alloy structures.

The plasmons leave a mark in the X-ray photoelectron and Auger electron spectrum (XPS and AES), which poses a challenge to the automatic spectra analysis. The results of the study are directly used to properly instruct the software to interpret the information correctly.

The application of this formalism to cases of experimental interest in AES and XPS, as well as the study of other forms of the system, as nanospheres and nanotubes is under way.

Appendix A.

According to the general formulation presented in the beginning of this paper and in Ref. [7], the different contribution to the induced potential in Eq. (5) are

$$F_{q_-}^{M,b} = \frac{-4\pi i q_-}{k^2}\left(\frac{1}{\epsilon(\omega)}-1\right)\left[e^{-i\kappa x_s}\left\{\frac{[1-e^{-i(\Omega-qu)t_0}]}{\Omega-qu-i\eta}-\frac{[1-e^{-i(\Omega+qu)t_0}]}{\Omega+qu-i\eta}\right\}\right.$$
$$\left.-2\frac{[1-e^{-i\Omega t_0}e^{-i\kappa z_0}]}{\Omega-i\kappa u}\right]$$

$$F_{q_-}^{M,s} = \frac{-4\pi i q_-}{k^2}\left(\frac{2}{\epsilon(\omega)+1}-1\right)\left[\frac{[1-e^{-i\Omega t_0}e^{-i\kappa z_0}]}{\Omega-i\kappa u}\right]$$

$$F_{q_+}^{M,b} = \frac{-4\pi i q_+}{k^2}\left(\frac{1}{\epsilon(\omega)}-1\right)\left[\frac{e^{-i\omega t_0}}{\omega-i\eta}(e^{iqz_0}-e^{-iqz_0})-2\frac{[e^{-\kappa z_0}e^{-i\omega t_0}]}{\omega-i\eta}\right]$$

$$F_{q_+}^{M,s} = \frac{-4\pi i q_+}{k^2}\left(\frac{2}{\epsilon(\omega)+1}-1\right)\left[\frac{[e^{-\kappa z_0}e^{-i\omega t_0}]}{\omega-i\eta}\right]$$

$$F_{q_-}^{V,s} = \frac{-4\pi i q_-}{k^2}\left(\frac{2}{\epsilon(\omega)+1}-1\right)\left[\frac{[1-e^{-i\Omega t_0}-e^{-i\kappa z_0}]}{\Omega-i\kappa u}-\frac{1}{\Omega+i\kappa u}\right]$$

$$F_{q_+}^{V,s} = \frac{4\pi i q_+}{k^2}\left(\frac{2}{\epsilon(\omega)+1}-1\right)\left[\frac{[e^{-\kappa z_0}e^{-i\omega t_0}]}{\omega-i\eta}\right]$$

References

[1] R.H. Ritchie, A.L. Marusak, Surf. Sci. 4 (1966) 234.
[2] F. Flores, F. Garcia-Moliner, J. Phys. C: Solid State Phys. 12 (1979) 907.
[3] R.H. Ritchie, Phys. Rev. A 106 (1957) 874.
[4] A.A. Lucas, M. Sunjic, Prog. Surf. Sci. 1 (1972) 75.
[5] T.L. Ferrell, P.M. Echenique, R.H. Ritchie, Solid State Commun. 32 (1979) 419.
[6] R. Nuñez, P.M. Echenique, R.H. Ritchie, J. Phys. C: Solid State Phys. 13 (1980) 4229.
[7] J.L. Gervasoni, N.R. Arista, Surf. Sci. 260 (1992) 329.
[8] J.L. Gervasoni, N.R. Arista, R.O. Barrachina, A. Gras-Marti, Nucl. Instr. Meth. B 67 (1992) 659.
[9] C.D. Denton, J.L. Gervasoni, R.O. Barrachina, N.R. Arista, Phys. Rev. A 57 (1998) 4498.
[10] R. Raether, Excitations of plasmons and interband transitions by electrons, Springer Tracts in Modern Physics, vol. 88, Springer, Berlin, 1980.
[11] K.D. Sevier, Low Energy Electron Spectrometry, Wiley-Interscience, New York, 1972.
[12] F. Yubero, S. Tougaard, Phys. Rev. B 71 (2005) 045414.
[13] J.L. Gervasoni, F. Yubero, Nucl. Instr. Meth. B 182 (2001) 96–101.
[14] H. Ibach, Electron Spectroscopy for Surface Analysis, Springer-Verlag, Berlin, 1977.
[15] O. Madelung, Phase Equilibria, Crystallographic and Thermodynamic Data of Binary Alloys, Springer-Verlag, Berlin, 1991.
[16] H. Luth, Surfaces and Interfaces of Solid Materials, Springer-Verlag, Berlin, 1995.
[17] D.P. Woodruff, T.A. Delchar, Modern Techniques of Surface Science, Cambridge Univ. Press, Great Britain, 1994.
[18] G.D. Mahan, in: Fiermans, Venik, Dekeyser (Eds.), Electron Spectroscopy of Solids, Plenum Press, New York, 1974.
[19] J.L. Gervasoni, L. Kovér, Surf. Interface Anal. 38 (2006) 652–656.
[20] J.L. Gervasoni, L. Kovér, J. Electron Spectrosc. Relat. Phenom. 161 (2007) 134–139.
[21] J.A. García Gallardo, J.L. Gervasoni, L. Kövér, J. Nanosci. Nanotechnol. 12 (12) (2012) 9271–9276.
[22] J.A. García Gallardo, J.L. Gervasoni, L. Kövér, Vacuum 84 (2010) 258–261.
[23] I. Abril, R. Garcia Molina, C.D. Denton, F.J. Perez-Perez, N.R. Arista, Phys. Rev. A 58 (1) (1998) 357.